Lawrence Berkeley National Laboratory
Recent Work

Title
THE LONG-TERM STABILITY OF AQUEOUS KOH FILMS ON PLATINUM

Permalink
https://escholarship.org/uc/item/9cr5p96h

Authors
Gyory, J.R.
Muller, R.H.

Publication Date
1986-11-01

eScholarship.org Powered by the California Digital Library
University of California

LBL-22523
Extended Abstract

Lawrence Berkeley Laboratory
UNIVERSITY OF CALIFORNIA

Materials & Molecular Research Division

RECEIVED
LAWRENCE
BERKELEY LABORATORY
FEB 9 1987
LIBRARY AND
DOCUMENTS SECTION

Presented at the 169th Meeting of the
Electrochemical Society, Boston, MA, May 4-9, 1986

THE LONG-TERM STABILITY OF AQUEOUS KOH FILMS ON PLATINUM

J.R. Gyory and R.H. Muller

November 1986

TWO-WEEK LOAN COPY
This is a Library Circulating Copy
which may be borrowed for two weeks.

Prepared for the U.S. Department of Energy under Contract DE-AC03-76SF00098

LBL-22523
extended
abstract
c.2

DISCLAIMER

This document was prepared as an account of work sponsored by the United States Government. While this document is believed to contain correct information, neither the United States Government nor any agency thereof, nor the Regents of the University of California, nor any of their employees, makes any warranty, express or implied, or assumes any legal responsibility for the accuracy, completeness, or usefulness of any information, apparatus, product, or process disclosed, or represents that its use would not infringe privately owned rights. Reference herein to any specific commercial product, process, or service by its trade name, trademark, manufacturer, or otherwise, does not necessarily constitute or imply its endorsement, recommendation, or favoring by the United States Government or any agency thereof, or the Regents of the University of California. The views and opinions of authors expressed herein do not necessarily state or reflect those of the United States Government or any agency thereof or the Regents of the University of California.

Abstract

White-light multiple beam interference is used to study the drainage of aqueous electrolytes from vertical polished metal plates. Initially, the change in profile agrees with that expected for viscous drainage. However, at long times, it deviates from that expected and the profiles become independent of time. Several equilibrium and dynamic models were investigated to explain this behavior. The long-term film profiles are best explained by a model based on long-range Van der Waals interactions. The magnitude of these interactions is characterized by the Hamaker constant. The magnitude and sign of Hamaker constants derived from film profile measurements agree well with those calculated from pure component dielectric data using Lifshitz' general theory of Van der Waals interactions.

Introduction

Liquid electrolyte films on metals are important in electrochemical systems involving gaseous reactants or products, such as fuel cells, gas evolution, and atmospheric corrosion. Also, an understanding of these films is necessary to determine the amount of electrolyte remaining on a surface when it is removed from solution for ex situ examination. The existence of thin liquid electrolyte films in electrode processes involving gaseous reactants was shown by Will (1). Bennion and Tobias (2) showed conclusively that a large fraction of the current for oxygen reduction in aqueous KOH is passed through a thin

film of electrolyte above the intrinsic meniscus of a partially submerged vertical electrode. In previous work, the thickness of these superminiscus thin films was measured using interference techniques and found to lie in the range of 0.1 to 1 μm (3). Deryagin and others (4,5) have also determined similar thicknesses and postulated that surface tension gradients were essential for maintaining these thin films. Work on film stability by Lightfoot and Ludviksson (6) has primarily concerned Marangoni films which tend to be much thicker (on the order of 50 μm). Despite these and other efforts no satisfactory explanation for the behavior of these supermeniscus thin electrolyte films has been found. It is the purpose of this work to study the stability of such films and to determine the forces responsible for their behavior.

Experimental

The object of the experiments was to create a thin supermeniscus film on a vertically oriented metal substrate. The thickness of this film was determined as a function of position on the metal substrate and time. These measurements were made on several substrates for various electrolytes and electrolyte concentrations.

Several different metal substrates have been used, they are: 1.) a 100 mm tall 40 mm wide 6 mm thick platinum plate where the back and sides were coated with an insulating non-reactive vinylidene fluoride resin, Kynar, produced by Pennwalt Corp., 2.) a 100 mm tall 100 mm wide 6 mm thick

platinum plate, and 3.) a 100 mm tall 40 mm wide 6 mm thick gold plated 316 LVM stainless steel plate where the back and sides were Kynar coated. The metal substrates were polished optically flat attaining less than 10 nm local roughness and less than 200 nm surface roll. The sides of the 100 mm by 100 mm platinum plate were rounded and polished and the back side was also polished in order to approximate an infinitely wide surface.

As shown by the cell diagram in figure 1, the polished metal substrate is positioned vertically in a Teflon cell. The cell, metal substrate and platinum mesh counter electrode are cleaned by soaking with concentrated nitric acid followed by 10% hydrogen peroxide. This treatment oxidizes any organic contaminants that may have been in the cell. In addition, the metal substrate and platinum counter electrode cause rapid dissociation of the hydrogen peroxide to water and oxygen. The vigorous bubbling of oxygen provides mechanical scrubbing of all interior surfaces which disslodges any small particles which are then removed from the cell upon drainage of the spent peroxide solution. Before electrolyte is added, the cell is rinsed several times with Harleco ultra pure, $\geq$ 10 MΩ/cm, water.

Electrolytic solutions are made only from Alfaproducts' ultra pure salts and Harleco ultra pure water. All solutions are mixed to the proper concentration in clean Teflon containers and stored under a nitrogen atmosphere. Before addition to the cell, all solutions are preelectrolyzed for at least 18 hours. The container used during preelectolysis is made of Teflon. The

current during preelectrolysis is passed between two platinum gauze electrodes are used and the current is controlled at 10 mA. Again, an inert nitrogen atmoshere is maintained during preelectrolysis.

Once both the cell and the electrolyte have been pretreated, the electrolyte is added to the cell so that the metal substrate is completely immersed, see figure 1a. Hydrogen is then evolved from the metal substrate to insure that any surface oxides produced during the pretreatment are reduced. Following hydrogen evolution, the boundary layer must be allowed to relax. Finally, the electrolyte is drained from the cell, leaving only a 6 mm deep liquid pool in which the bottom of the metal substrate is immersed, see figure 1b. During the lowering of the liquid level, the electrolyte volume is replaced by high-purity nitrogen that is water saturated with solution of the same concentration used in the cell. As the electrolyte film drains, its thickness is recorded by white-light interference at the optimum angle of incidence (9) with a time-lapse 16 mm movie camera. Thin film interference is a noninvasive technique which is very sensitive to thicknesses on the order 100 to 10,000 Angstroms.

Results

Film profiles derived from interference pictures of draining 1 N KOH on platinum are illustrated in figure 2 for drainage times (time since lowering of liquid level) of 1, 3, and 24 hours. The upper portion of the 3 hour profile

illustrates the parabolic shape expected when only viscous and gravitational forces are considered (see the discussion section concerning Jeffrey's equation). For times greater than 24 hours, the profile is constant with time. The film thickness at two levels above the liquid is shown in figure 3 to initially decrease with the inverse square root of time. But, at about 18 hours the thickness deviates from this behavior and becomes time invariant to 30 days (other observations have shown the same behavior until terminated at 60 days). The time-invariant profiles for 1M KOH on Pt, 1M KOH on Au, and 1M $NaClO_4$ on Pt are shown in figures 4, 5, and 6 respectively. Figure 7 shows that as electrolyte concentration increases, the time-invariant profile thickness increases.

Discussion

When fluid drains by gravity from the surface of a vertical plate, Jeffreys (7) showed that at any time, t, the liquid film thickness, δ, is given by:

$$\delta = \sqrt{\frac{\mu z}{\rho g t}}, \qquad (1)$$

where z is the distance from the film attachment point downward, and μ, ρ, and g are the liquid viscosity, liquid density, and the gravitational constant respectively. Tallmadge (8), among others, has introduced corrections to this equation that take capillarity and the speed of bulk liquid withdrawl into account. At long drainage times, these equations converge to

Jeffrey's, *i.e.*, the film thickness is inversely proportional to the square root of time and approaches zero as time approaches infinity. As is shown in figure 3 for aqueous KOH on platinum, we have observed appreciable deviation from this behavior. And contrary to the above equation, for long times we have observed that these films achieve a time-independent profile. Numerical curve fitting of many different time-invariant profiles reveals that the film thickness, δ, is proportional to the inverse cube root of the distance above the bulk liquid level, h, ie,

$$\delta \propto \frac{1}{\sqrt[3]{h}} \quad . \tag{2}$$

Models investigated to explain the long-term stability of these films lie in two categories, depending on whether they are based on a dynamic steady state or an equilibrium. Dynamic models require the assumption of fluid motion, *e.g.*, driven by surface tension gradients or vapor pressure gradients. These models were abandoned because a source of energy to maintain sufficient temperature or concentration differences over extended periods in a sealed isothermal cell could not be identified.

Several equilibrium models were also investigated. The electrical repulsion between the double layer at the metal/electrolyte interface and the double layer at the electrolyte/vapor interface predicts a functionality other than that observed. Also, as electrolyte concentration is increased, we would expect film thicknesses to decrease as a result of double-layer compression.

However, as shown in figure 7, increasing electrolyte concentrations were found to result in larger, not the predicted smaller film thicknesses.

Surface-active impurities were also considered as a possible stabilizing influence. It is well known that as a liquid film drains surfactants can cause the immobilization of the liquid/vapor interface. However, the film interior continues to drain viscously. Therefore, immobilized liquid-gas interfaces, resulting from the accumulation of surface-active impurities, will result in slower drainage rates, but the film thickness will still approach zero, or at most the thickness of a monolayer of surfactant, as time approaches infinity.

The only model investigated which predicts a film profile functionality in agreement with experimental observations (see equation 2) is one based on long-range Van der Waals interactions. In 1937 Hamaker (10) showed that long-range Van der Waals interactions between two semi-infinite phases interacting through a thin film third phase manifest themselves as an effective interfacial force that is proportional to the inverse cube of the film thickness. Deryagin proposed that this interfacial force could be treated as an effective change in pressure within the thin film, and he termed this pressure change the disjoining pressure(11). As an example, if the internal film pressure is higher than the external pressure, *i.e.*, the disjoining pressure is possitive, then there will be an apparent repulsive force between the interfaces, and if the internal film pressure is lower than the external pressure, *i.e.*, the disjoining pressure is negative, then there will be an apparent attractive force

between the interfaces. Another way of summarizing this result is: the pressure within the thin film will increase if the net interfacial force is repulsive, or conversely decrease if the net interfacial force is attractive. By equating the hydrostatic pressure within the film to the negative of the disjoining pressure within the film the film thickness, δ, as a function of the height, h, above the bulk liquid level can be derived and is found to be;

$$\delta = - \sqrt[3]{\frac{A}{6 \pi \rho g h}}, \tag{3}$$

where A is the Hamaker constant and ρ and g are the liquid density and the gravitational constant respectively. A calculated profile with $A = -1 \times 10^{-11}$ ergs is shown in figure 4 together with measured data for 1M KOH on platinum. Figures 5 and 6 show similar results for 1M KOH on Au and 1M $NaClO_4$ on Pt. The Hamaker constants derived from these film profiles are shown in Table 1.

No measured or calculated values of the Hamaker constant for the systems studied here have been reported. Furthermore, very little attention has been given to either metals or electrolytic solutions. This appears largely due to the complexity involved in treating these systems. In the late 1950's, Lifshitz (12) introduced a general theory for the treatment of Van der Waals interactions. Lifshitz' theory was the first to be quantum mechanically correct. Also, another feature of this theory is that one only needs to know data derived from measurements on pure components. Unfortunately, the data

required are the dielectric functions of each individual phase, ϵ_1, ϵ_2, and ϵ_3, (see figure 8) measured for all imaginary frequencies, ξ, from 0 to ∞. From Lifshitz' theory, the Hamaker constant is given by;

$$A_{132} = \sum_{n=0}^{\infty}{}' \sum_{j=0}^{\infty} \frac{1}{j^3} \left(\frac{(\epsilon_1(i\,\xi_n)-\epsilon_3(i\,\xi_n))\,(\epsilon_2(i\,\xi_n)-\epsilon_3(i\,\xi_n))}{(\epsilon_1(i\,\xi_n)+\epsilon_3(i\,\xi_n))\,(\epsilon_2(i\,\xi_n)+\epsilon_3(i\,\xi_n))} \right)^j, \qquad (4)$$

where the prime on the first summation denotes the n=0 term is to be multiplied by $\frac{1}{2}$, i is the imaginary unit, and ξ_n is the discrete frquency at which the dielectric function is evaluated (see equation 5).

$$\xi_n = \frac{3\,k\,T\,n}{2\,h}, \quad n = 0, 1, 2, \cdots \infty \qquad (5)$$

In equation 5, k and h are Boltzman's and Plank's constants respectively and T is the absolute temperature.

The main difficulty in applying equation 4 is that the dielectric function of all phases must be known over a large portion of the spectrum. Assumptions can be made concerning the functionality of $\epsilon(i\,\xi)$ which make it possible to simplify and integrate equation 4. For a review of some of these efforts see Israelachvili (13). Unfortunately, metals and electrolytic solutions do not readily lend themselves to simplifying assumptions of this sort. Therefore, Lifshitz' full expression must be evaluated in order to calculate the Hamaker constant for systems involving these materials. Some means of determining the dielectric function of the three pure phases must be used. Generally, absorption spectra of the pure phases can be used in conjunction with one of

the Kramers-Kronig transformations to generate the dielectric function over all imaginary frequencies. For several methods of achieving this see Hough and White (14) and Parsegian and Weiss (15).

Calculated Hamaker constants using the method and data of Parsegian and Weiss appear in Table 2. The calculated value for the Gold/Water/Vacuum system shows good agreement with the Hamaker constant derived from film profile measurements for the Gold/1 N KOH/Air system reported in Table 1. Both values are negative indicating that the effective interfacial force is repulsive. The calculated Hamaker constant for the Gold/Water/Gold system reported in table 2 is positive denoting the force between the surfaces is attractive. Its value agrees well with the value reported in table 3 that was derived from a direct force measurement made by Deryagin (16). Also appearing in table 3 is the Hamaker constant derived from a direct force measurement for the Quartz/Tetradecane/Air system. It is shown as an example of other negative Hamaker constant systems, ie, the force between the interfaces is repulsive.

If we analyze the mathematical properties of equation 4 we can gain some insight into the sign and magnitude of the calculated Hamaker constant. First, at each term of the summation over n, the contribution to the Hamaker constant is governed by two ratios made up of the difference divided by the sum of the dielectric functions of two individual phases (see equations 6 and 7). Hough and White (14) demonstrate the following; 1) at

$n = 0$, (0 frequency), $\epsilon(i\,\xi_n)$ is equal to the static dielectric constant of that phase, and 2) as n increases, *i.e.*, as frequency increases, ϵ decreases monotonically until it reaches 1 at large n. Therefore, ϵ is always positive and greater than or equal to 1. Therefore, if $\epsilon_1 > \epsilon_3 > \epsilon_2$, the product in equation 4 will be negative. However, if ϵ_3 is either larger or smaller than both ϵ_1 and ϵ_2, the product will be positive. In other words, if the dielectric properties of the thin film phase are intermediate between the dielectric properties of the bounding phases the surfaces will effectively repel one another. Conversely, if the dielectric properties of the thin film phase are larger than both or smaller than both the bounding phases, the interfaces will effectively attract one another.

By comparing values of the Hamaker constants reported in tables 1-3 one quickly recognizes that systems involving platinum or gold exhibit Hamaker constants of the order 1×10^{-12} ergs. On the other hand, Hamaker constants for systems involving three dielectric phases such as the quartz/tetradecane/air system tend to have Hamaker constants of the order 1×10^{-14} or smaller, although only one of these systems is presented here, this trend is readily observed by comparing values reported in Israelachvili (13) or Hough and White (14). The basis for this two order of magnitude difference in the Hamaker constant is shown in figure 9. This figure compares the dielectric functions for gold, water, and tetradecane which were calculated from fitted absorption spectra by the method and data of Parsegian and

Weiss (15). Figure 9 clearly illustrates the relatively large dielectric function for gold as compared to water or tetradecane. Because the dielectric function for gold is so large, each term of equation 4 will be much larger for systems involving the gold/water interaction than for systems involving the tetradecane/water interaction. Therefore, since in general metals exhibit a larger dielectric function than do dielectrics, systems involving a metal/dielectric interaction will have larger Hamaker constants than will systems involving only dielectric/dielectric interactions.

Presently, calculations have not been completed on the effect of dissolved salts on the total Van der Waals interaction. However, a qualitative arguement follows that suggests that Van der Waals interactions can also account for the increasing film thickness with increasing electrolyte concentration. It is known that adding KOH to water increases the refractive index in the visible frequencies, this would correspond to increasing the dielectric function. Each term of equation 4 is the product of two ratios and these ratios are;

$$R_1 = \frac{\epsilon_1 - \epsilon_3}{\epsilon_1 + \epsilon_3} , \tag{6}$$

$$R_2 = \frac{\epsilon_2 - \epsilon_3}{\epsilon_2 + \epsilon_3} , \tag{7}$$

where R_1 and R_2 are frequency dependent as is explicitly shown in equation 4, and phase 1 is metal, phase 2 is air, and phase 3 is the thin electrolyte film (see figure 8). Recognizing that for most frequencies of importance ,the near

infrared through the far ultraviolet, $\epsilon_1 >> \epsilon_3$ (see figure 9), therefore a small change in ϵ_3 caused by the addition of KOH to the thin electrolyte film phase will cause a relatively small decrease in the magnitude of R_1. However, because ϵ_2 and ϵ_3 are comparable through out this frequency range (see figure 9) a small increase in ϵ_3 will result in a significant increase in the magnitude of R_2. Consequently, the product of R_1 and R_2 will show an overall increase in magnitude when the dielectric function of the thin film phase is increased by the addition of KOH.

Conclusions

We have demonstrated that thin stable superminiscus films on metals do exist, and for KOH on platinum the equilibrium thickness of these films is of the order 0.1 μm. Also, the behavior of these films is not described by double-layer interaction or by surface-active impurities. A model based on long-range Van der Waals interactions resulting in a repulsive force between the metal/liquid interface and the liquid/air interface agrees with the experimental findings. Finally, values of the Hamker constant derived from film profiles agree well with values calculated from measured dielectric data of each individual phase using Lifshitz' general theory of Van der Waals interactions. Future work will include: 1.) calculating the effect of electrolyte concentration on the Hamaker constant, 2.) including the Van der Waals interaction in the hydrodynamic equations to calculate the rate of drainage prior to

achieving time-independent profiles, and 3.) prediction of an equilbrium profile followed by experimental measurement for a system that has not previously been studied.

Acknowledgment

This work was supported by the Director, Office of Energy Research, Office of Basic Research, and Materials Sciences Division of the US Department of Energy under Contract No. DE-AC03-76SF00098.

References

1. F. G. Will, *J. Electrochem. Soc.*, **110**, 145 (1963).
2. D. N. Bennion and C. W. Tobias, *J. Electrochem. Soc.*, **113**, 589 (1966).
3. R. H. Muller, *J. Electrochem. Soc.*, **113**, 943 (1966).
4. B. V. Deryagin, et al., *Colloid J. of the USSR*, **23**, 535 (1961).
5. S. F. Chernyshov, et al., *Elektrokhimiya*, **6**, 949 (1970).
6. V. Ludviksson, and E. N. Lightfoot, *AIChE J.*, **17**, 1166 (1971).
7. H. Jeffreys, *Proc. Camb. Phil. Soc.*, **26**, 204 (1930).
8. J. A. Tallmadge, *J. Phys. Chem.*, **75**, 583 (1971).
9. R. H. Muller, *J. Opt. Soc. Amer.*, **54**, 419 (1964).
10. H. C. Hamaker, *Physica*, **4**, 1058 (1937).
11. B. V. Deryagin, and M. Kussakov, *Acta Physicochimica U.R.S.S.*, **10**, 25 (1939).
12. E. M. Lifshitz, *Soviet Physics JETP*, **2**, 73 (1956).
13. J. N. Israelachvili, *Intermolecular and Surface Forces*, Academic Press, NY (1985).
14. D. B. Hough and L. R. White, *Adv. Col. Int. Sci.*, **14**, 3 (1980).
15. V. A. Parsegian and G. H. Weiss, *J. Col. Int. Sci.*, **81**, 285 (1981).
16. B. V. Deryagin, Y. I. Rabinovich, and N. V. Churaev, *Nature*, **272**, 313 (1978).

TABLE 1

Hamaker Con. Derived From Film Profile	
Gold / 1 N KOH / Air	-2×10^{-12} ergs
Platinum / 1 N KOH / Air	-10×10^{-12} ergs
Platinum / 1 N $NaClO_4$ / Air	-1.7×10^{-12} ergs

TABLE 2

Hamaker Constant; Calculated	
Gold / Water / Vacuum	-0.97×10^{-12} ergs
Gold / Water / Gold	2.7×10^{-12} ergs

TABLE 3

Hamaker Con. Derived From Force Measurement	
Gold / Water / Gold	4.0×10^{-12} ergs
Quartz / $C_{14} H_{30}$ * / Air	-0.05×10^{-12} ergs

* $C_{14} H_{30}$ = Tetradecane

Figure Captions

Figure 1: Cross section of cell for observing thin liquid films on metal substrates, (a) filled, and (b) drained.

Figure 2: Profiles for 1M KOH on platinum for different times after drainage. A) 1 hour, B) 3 hours, and C) 24 hours. (For all times greater than 24 hours the film profile was constant.) Coordinate definitions for δ, h, and z are also shown.

Figure 3: Drainage of 1M KOH on Pt observed at 7 cm. (points A) and 1 cm. (points B) above the bulk liquid level. The lines shown are calculated for viscous drainage from Jeffrey's equation, eq. 1, with $\rho = 1.1$ gm/cm^3 and $\mu = 1.0$ centipoise.

Figure 4: Measured film thicknesses of 1M KOH on Pt after 24 hours of drainage (data points P and S are derived from interference colors of p and s polarized light), and film profile predicted by eq. 3 (solid line) with $A = -1 \times 10^{-11}$ ergs.

Figure 5: Measured film thicknesses of 1M KOH on Au after 96 hours of drainage (data points P and S are derived from interference colors of p and s polarized light), and film profile predicted by eq. 3 (solid line) with $A = -2 \times 10^{-12}$ ergs.

Figure 6: Measured film thicknesses of 1M $NaClO_4$ on Pt after 48 hours of drainage (data points P and S are derived from interference colors of p and s polarized light), and film profile predicted by eq. 3 (solid line) with $A = -1.7 \times 10^{-12}$ ergs.

Figure 7: Effect of concentration on equilibrium film thickness at 5 cm. above the bulk liquid level for KOH on Pt (A), KOH on Au (B), and $NaClO_4$ on Pt (C).

Figure 8: Numbering of substrate, film, and gas phases for dielectric functions, ϵ, and Hamaker constant, A_{132}.

Figure 9: Dielectric functions for gold, tetradecane, and water as a function of frequency (hertz). The DC ($\xi = 0$) value for water is 80 and for tetradecane is 2.0 (20 ° C).

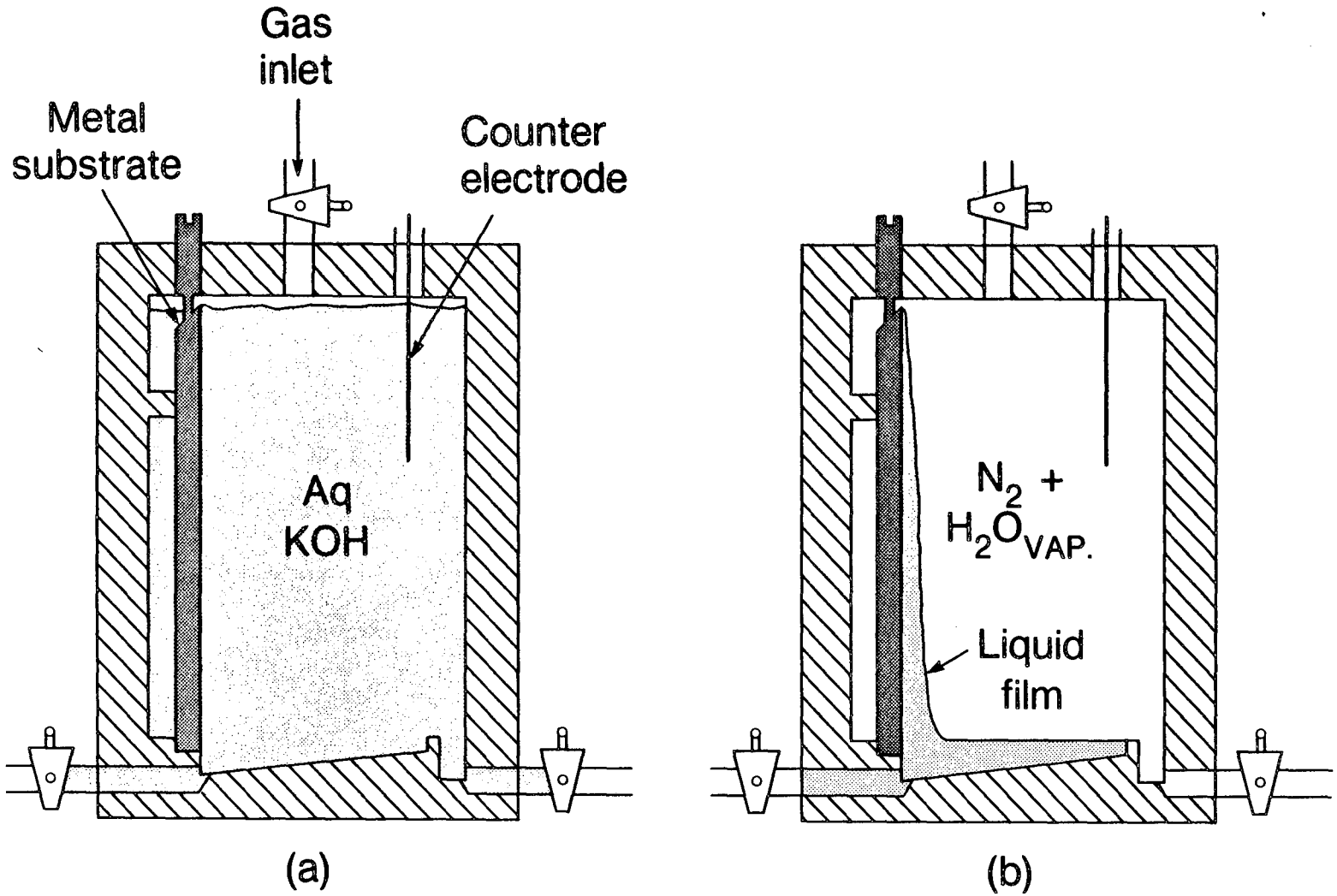

XBL 8611-9959 A

Fig. 1

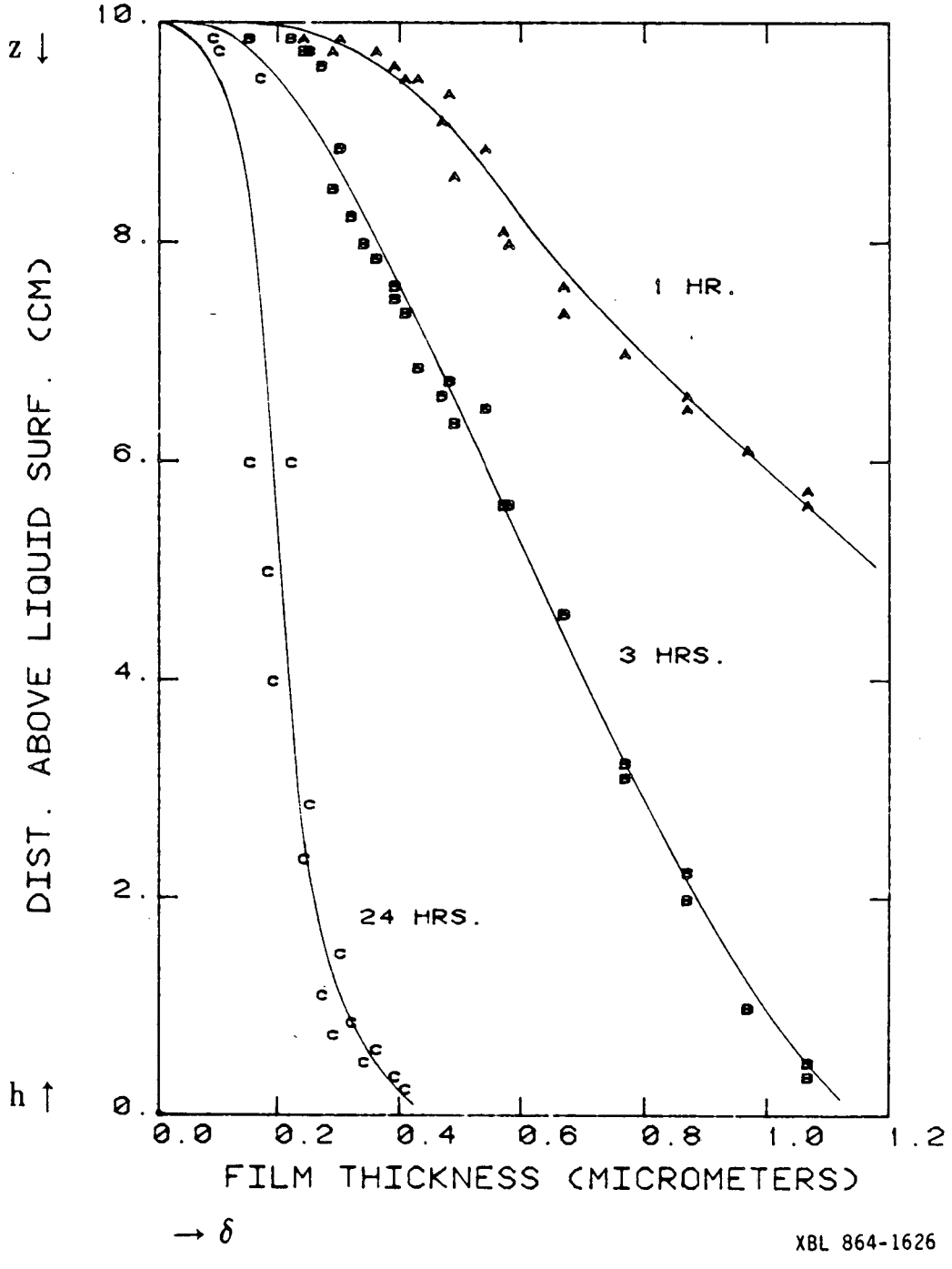
z ↓
10.
8.
6.
4.
2.
0.
DIST. ABOVE LIQUID SURF. (CM)
h ↑
1 HR.
3 HRS.
24 HRS.
0.0
0.2
0.4
0.6
0.8
1.0
1.2
FILM THICKNESS (MICROMETERS)
→ δ
XBL 864-1626

Fig. 2

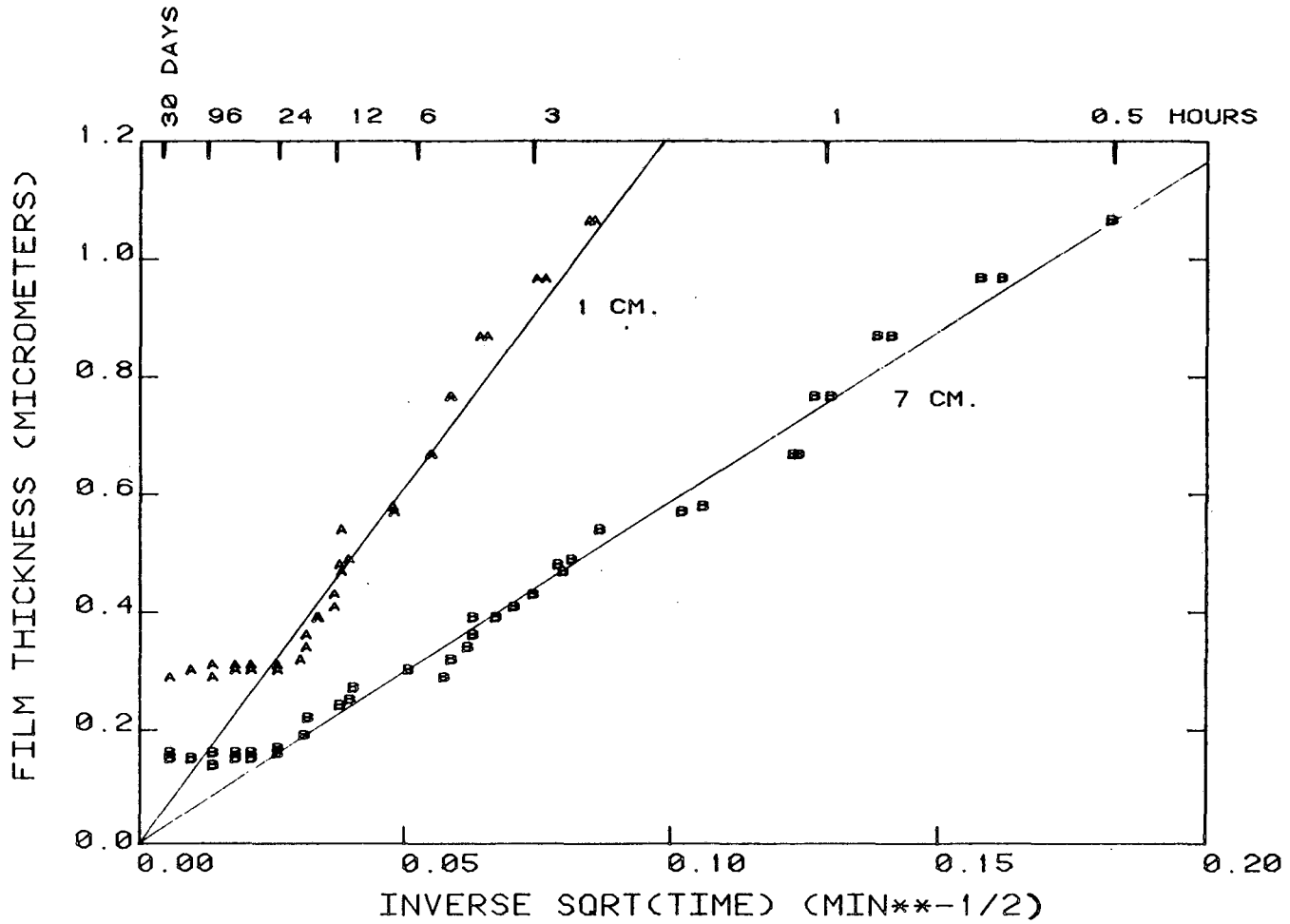

XBL 864-1627

Fig. 3

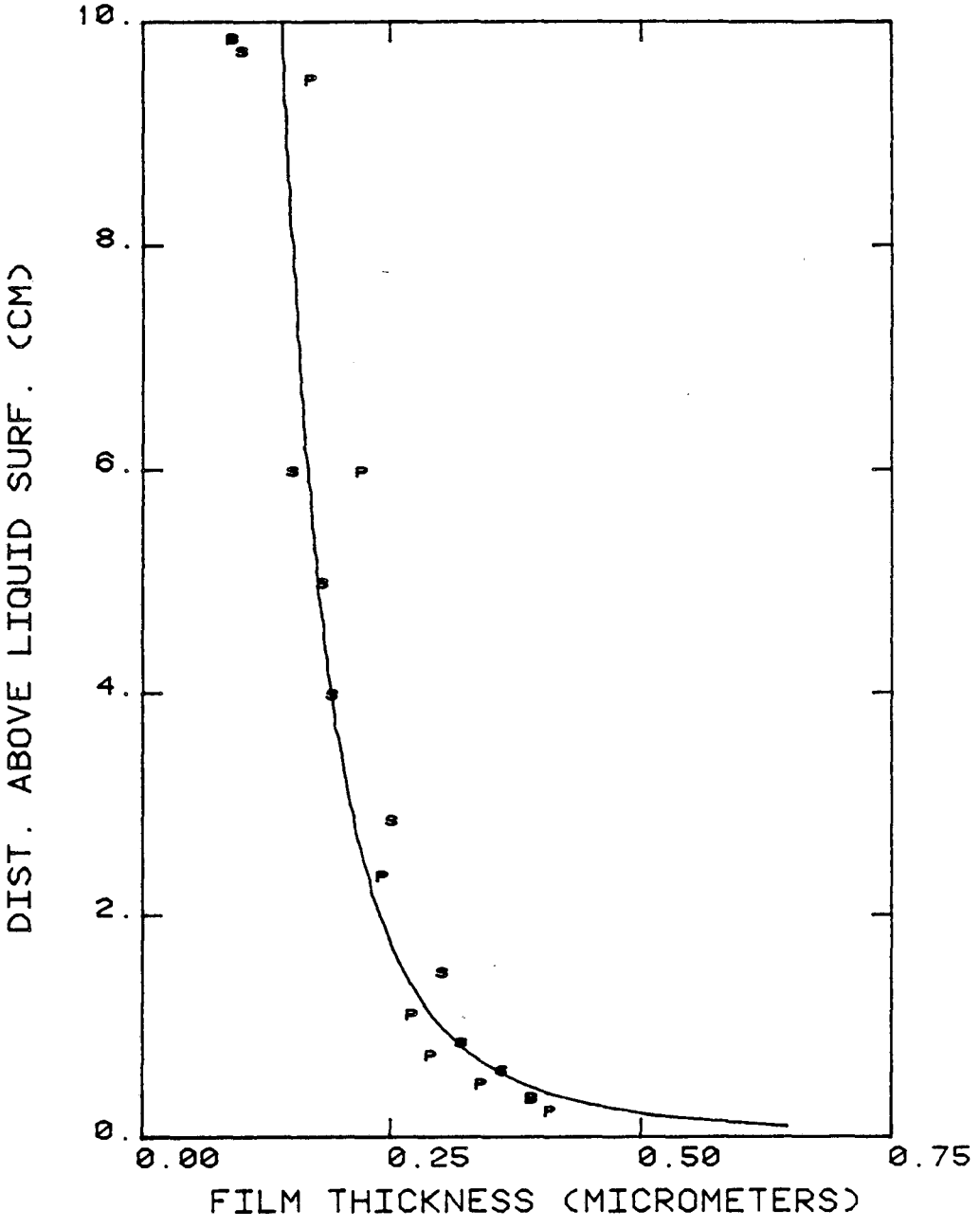

XBL 864-1629

Fig. 4

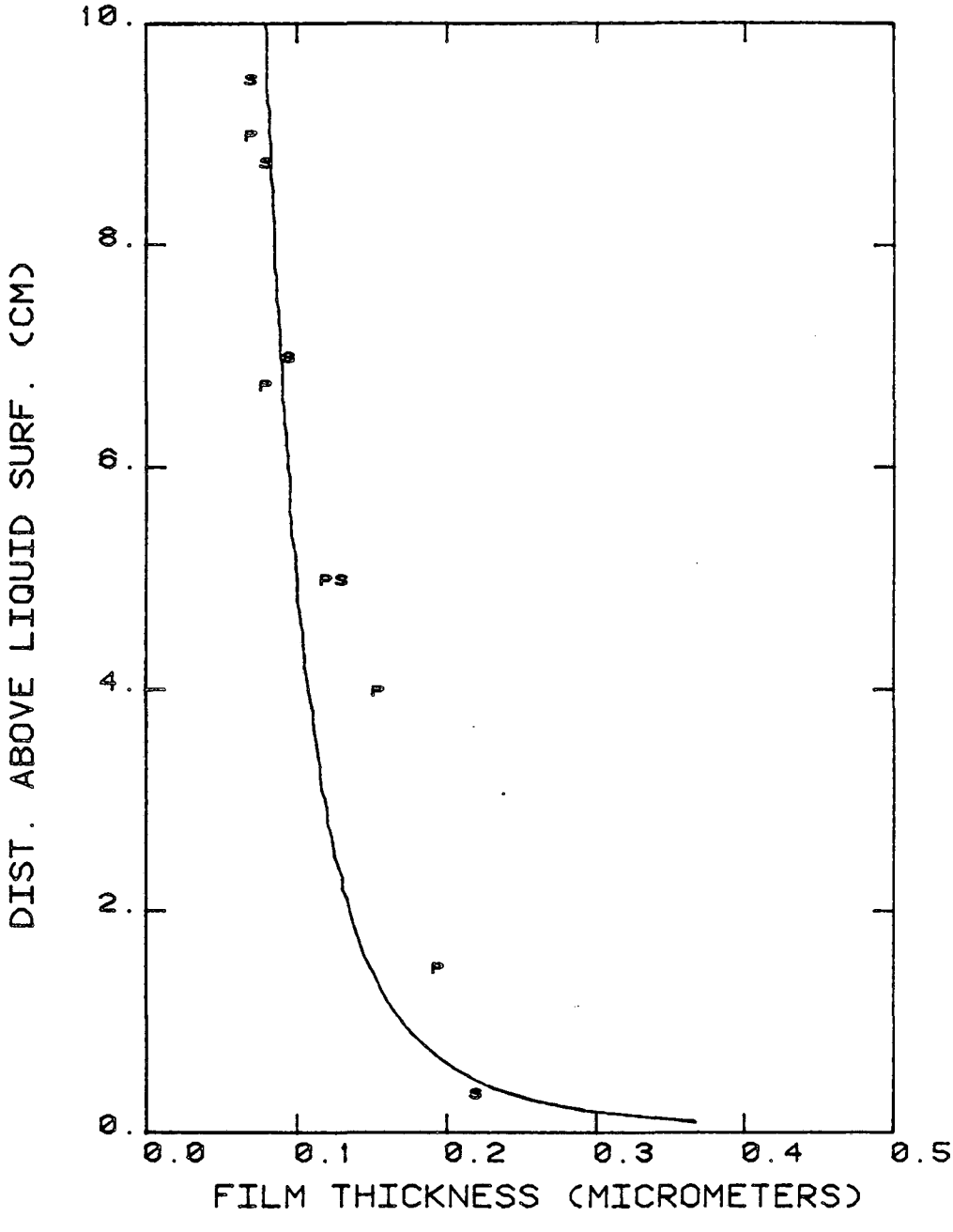

XBL 864-1630

Fig. 5

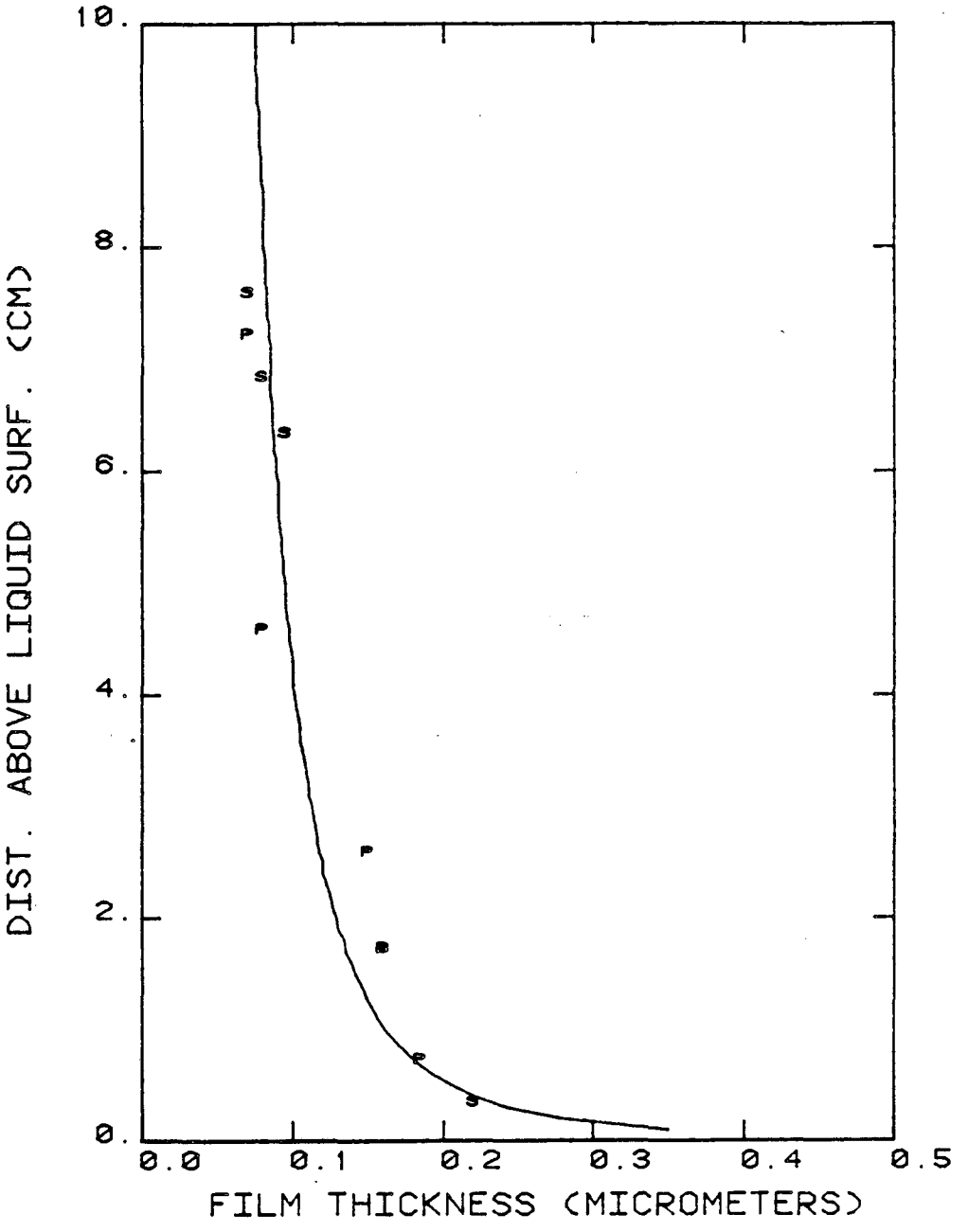

XBL 864-1631

Fig. 6

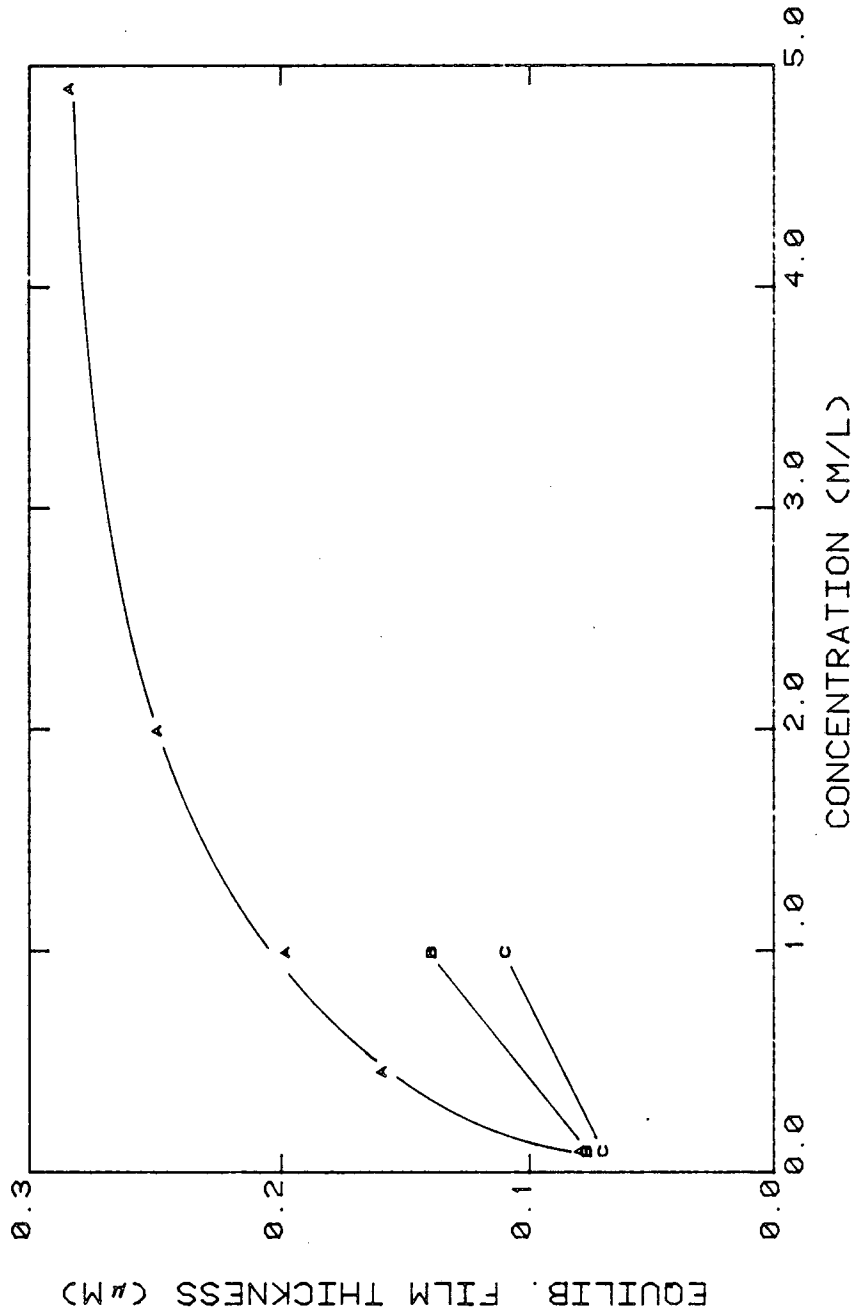

XBL 864-1628

Fig. 7

VAN DER WAALS INTERACTION

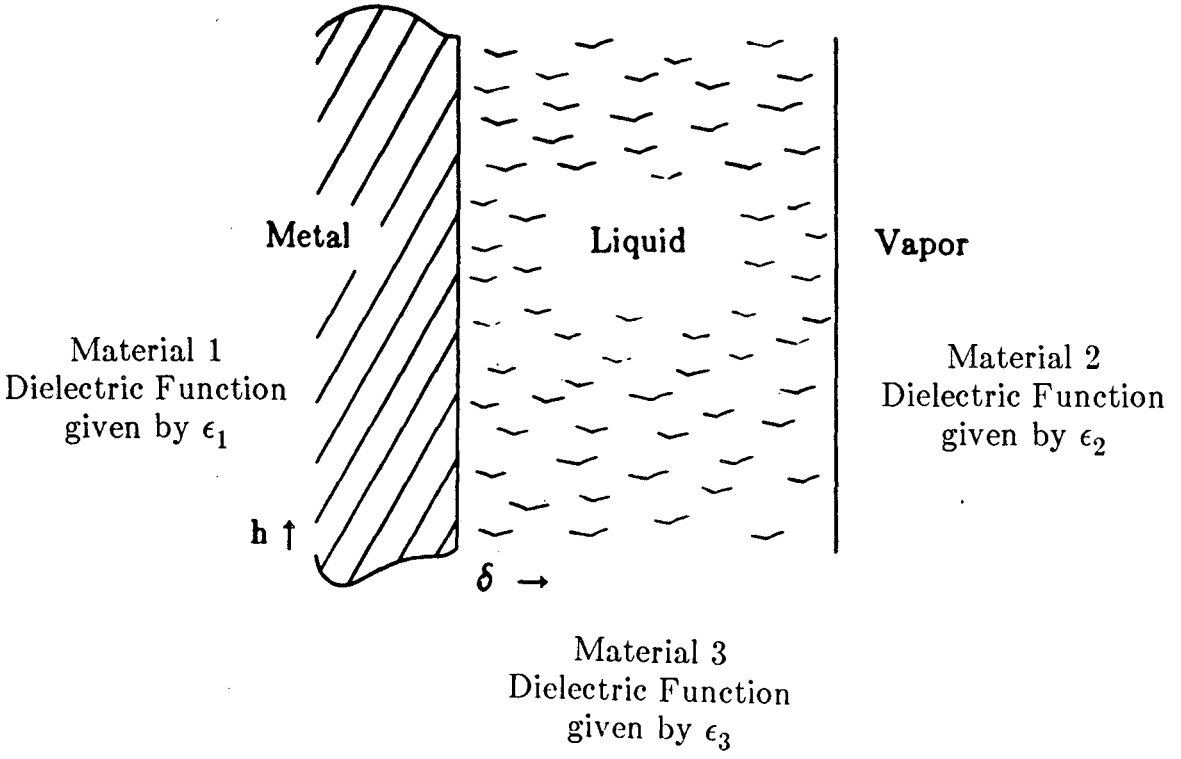

XBL 869-3350

Fig. 8

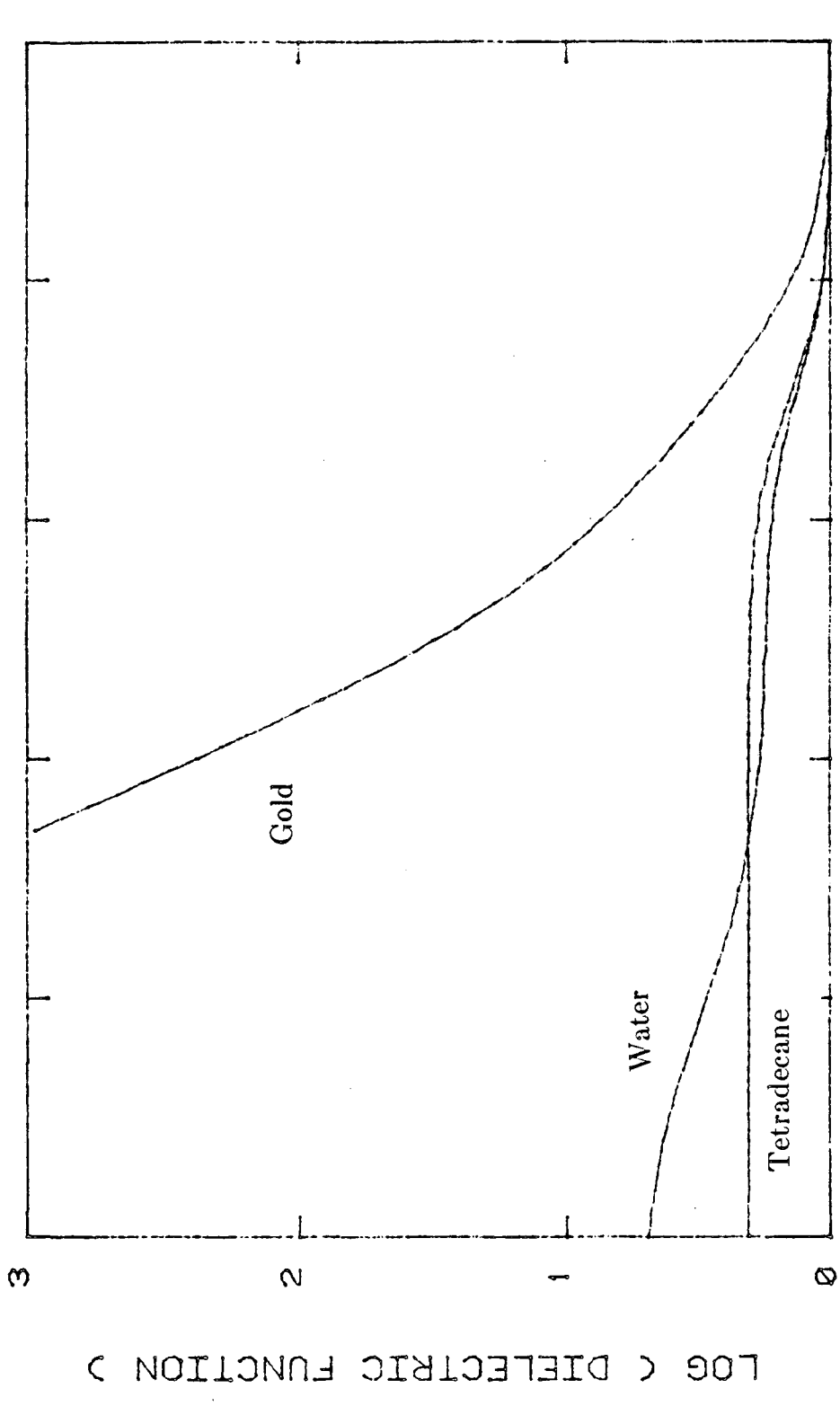

XBL 8611-4776

Fig. 9

This report was done with support from the Department of Energy. Any conclusions or opinions expressed in this report represent solely those of the author(s) and not necessarily those of The Regents of the University of California, the Lawrence Berkeley Laboratory or the Department of Energy.

Reference to a company or product name does not imply approval or recommendation of the product by the University of California or the U.S. Department of Energy to the exclusion of others that may be suitable.

LAWRENCE BERKELEY LABORATORY
TECHNICAL INFORMATION DEPARTMENT
UNIVERSITY OF CALIFORNIA
BERKELEY, CALIFORNIA 94720